CrossMark
← click for updates

A highly selective and sensitive fluorescent turn-on Al^{3+} chemosensor in aqueous media and living cells: experimental and theoretical studies†

In Hong Hwang,[a] Ye Won Choi,[a] Kyung Beom Kim,[a] Gyeong Jin Park,[a] Jae Jun Lee,[a] LeTuyen Nguyen,[b] Insup Noh[b] and Cheal Kim*[a]

A highly selective and sensitive fluorescent chemosensor (**1**) based on a 2-aminobenzoic acid Schiff base has been synthesized in one step. The binding properties of **1** with metal ions were investigated by fluorescence, UV-vis, ^{1}H NMR and electrospray ionization mass spectra. This sensor exhibited enhanced fluorescence in the presence of Al^{3+} in aqueous solution and also in living cells. The sensing mechanism of **1** toward Al^{3+} was explained by DFT/TDDFT calculations. The binding constant was determined to be 3.1×10^8 M^{-1} which is one of the highest binding affinities among such simple Schiff bases for Al^{3+} in buffer solution. The calibration curve for the analytical performance of Al^{3+} was found to be linear over a concentration range with a very low detection limit of 290 nM (3σ).

1. Introduction

The development of selective and sensitive chemosensors for the detection of metal ions has received considerable attention because of their important roles in medicine, living systems and the environment.[1–7] Among metals, aluminum is the third most prevalent metallic element in the Earth. People are widely exposed to aluminum because of its widespread use in food additives, aluminum-based pharmaceuticals and storage/cooking utensils.[8–13] The World Health Organization (WHO) prescribed the average human intake of aluminum to be around 3–10 mg day^{-1} and limited its drinking water concentration to 7.41 μM. Tolerable weekly aluminum intake in the human body is estimated to be 7 mg kg^{-1} body weight.[14–16] The superfluous ingestion of aluminum influences the absorption of calcium in the bowel, causing softening of the bone, atrophy and even aberrance, and also affects the absorption of iron in blood, causing anemia. In addition, the toxicity of aluminum causes damage to the central nervous system, is suspected to be involved in neurodegenerative diseases such as Alzheimer's and Parkinson's, and is responsible for intoxication in hemodialysis patients.[17–19]

In recent years, much effort has been devoted to design various chemosensors specific for Al^{3+} detection.[20–61] However, many of them have suffered from the cost of synthesis, the number of synthesis steps, selectivity, binding constants, detection limits, use of harmful organic solvents, and poor water solubility. Therefore, it is necessary to develop new sensors for selectively detecting Al^{3+} in aqueous solution. To increase the water solubility, we used 2-aminobenzoic acid with a carboxylic group acting as a hydrophilic character. To the best of our knowledge, very few studies have been reported on the use of aminobenzoic acid as a fluorescent chemosensor for the detection of metal ions.[32,62–65]

Herein, we report an aminobenzoic acid-based Schiff base **1** as a highly selective and sensitive fluorescent chemosensor for Al^{3+}. **1** showed one of the highest binding affinities ($K_a = 3.0 \times 10^8$ M^{-1}) among such simple Schiff bases for Al^{3+} in aqueous solution and quite a low detection limit (2.9×10^{-7} M) of a nanomolar concentration level.

2. Experimental section

2.1. Materials and instrumentation

All the solvents and reagents (analytical grade and spectroscopic grade) were obtained from Sigma-Aldrich and used as received. The Live/Dead assay (LIVE/DEAD® Viability/Cytotoxicity Kit) kit was purchased from Life Technologies Company. ^{1}H NMR measurements were performed on a Varian 400 MHz spectrometer and chemical shifts were recorded in ppm. Electrospray ionization mass spectra (ESI-MS) were collected on a Thermo Finnigan

a Department of Fine Chemistry and Department of Interdisciplinary Bio IT Materials, Seoul National University of Science and Technology, Seoul 139-743, Korea. E-mail: chealkim@seoultech.ac.kr; Fax: +82-2-973-9149; Tel: +82-2-970-6693

b Department of Chemical and Biomolecular Engineering, and Convergence Program of Biomedical Engineering and Biomaterials, Seoul National University of Science & Technology, Seoul 139-743, Republic of Korea

† Electronic supplementary information (ESI) available. See DOI: 10.1039/c5nj02334c

(San Jose, CA, USA) LCQ™ Advantage MAX quadruple ion trap instrument. Elemental analysis for carbon, nitrogen, and hydrogen was carried out by using a Flash EA 1112 elemental analyzer (thermo) in the Organic Chemistry Research Center of Sogang University, Korea. Absorption spectra were recorded at 25 °C using a Perkin Elmer model Lambda 2S UV/vis spectrometer. Fluorescence measurements were performed on a Perkin Elmer model LS45 fluorescence spectrometer.

2.2. Synthesis of the fluorescence sensor 1

A solution of 2-aminobenzoic acid (0.14 g, 1 mmol) in ethanol was added to a solution containing 4-(diethylamino)-2-hydroxybenzaldehyde (0.19 g, 1 mmol) in ethanol and the mixture was stirred for 5 min. Then, two drops of HCl were added into the reaction solution and it was stirred for 3 h at room temperature. The solvent was evaporated and a bright yellow product was recrystallized from acetonitrile. The yield: 0.23 g (74.3%). ^{1}H NMR (DMSO-d_6, 400 MHz) δ: 8.72 (s, 1H), 7.93 (d, 1H, J = 7.6 Hz), 7.58 (d, 2H, J = 6.8 Hz), 7.44 (d, 1H, J = 8.8 Hz), 7.29 (m, 1H, J = 7.6 Hz), 6.41 (d, 1H, J = 8.4 Hz), 6.39 (s, 1H), 3.45 (q, 4H, J = 6.8 Hz), 1.14 (t, 6H, J = 7.0 Hz). ESI-mass $m/z\,[\mathrm{M}-\mathrm{H}^+]^-$: calcd, 311.14; found, 311.33. Anal. calcd for $C_{18}H_{20}N_2O_3$ (312.15): C, 69.21; H, 6.45; N, 8.97. Found: C, 69.60; H, 6.30; N, 8.70%.

2.3. Fluorescence and UV-vis measurements

For fluorescence measurements, sensor **1** (1.6 mg, 0.005 mmol) was dissolved in methanol (5 mL) and 30 μL of sensor **1** (1 mM) were diluted with 2.97 mL bis-tris buffer (10 mM, pH 7.0, water : CH$_3$OH = 1 : 1 (v/v)) to make the final concentration of 10 μM. Al(NO$_3$)$_3$·9H$_2$O (37.5 mg, 0.1 mmol) was dissolved in methanol (5 mL). 1.5–28.5 μL of the Al^{3+} solution (20 mM) were transferred to each sensor solution (10 μM) prepared above. After mixing them for a few seconds, fluorescence spectra were obtained at room temperature.

For UV-vis measurements, all experimental conditions were identical as above. 1.5–21 μL of the Al^{3+} solution (10 mM) were transferred to each sensor solution (10 μM) prepared above. After mixing them for a few seconds, UV-vis spectra were taken at room temperature.

2.4. Job plot measurements

Sensor **1** (1.6 mg, 0.005 mmol) was dissolved in methanol (5 mL). 30, 27, 24, 21, 18, 15, 12, 9, 6, 3 and 0 μL of the sensor **1** solution were taken and transferred to vials. Each vial was diluted with bis-tris buffer (10 mM, pH 7.0, water : CH$_3$OH = 1 : 1 (v/v)) to make a total volume of 2.97 mL. Al(NO$_3$)$_3$·9H$_2$O (1.9 mg, 0.005 mmol) was dissolved in methanol (5 mL). 0, 3, 6, 9, 12, 15, 18, 21, 24, 27 and 30 μL of the Al(NO$_3$)$_3$ solution were added to each diluted sensor **1** solution. Each vial had a total volume of 3 mL. After shaking the vials for a few seconds, fluorescence spectra were taken at room temperature.

2.5. NMR titration

For ^{1}H NMR titration of sensor **1** with Al^{3+}, four NMR tubes of sensor **1** (31.2 mg, 0.1 mmol) dissolved in DMSO-d_6 (700 μL) were prepared and then four different concentrations

(0, 0.02, 0.05 and 0.1 mmol) of Al(NO$_3$)$_3$·9H$_2$O dissolved in DMSO were added to each solution of sensor **1**. After shaking them for a minute, ^{1}H NMR spectra were recorded at room temperature.

2.6. Competition with other metal ions

Sensor **1** (1.6 mg, 0.005 mmol) was dissolved in methanol (5 mL) and 30 μL of sensor **1** (1 mM) were diluted with 2.97 mL bis-tris buffer (10 mM, water : CH$_3$OH = 1 : 1 (v/v)) to make the final concentration of 10 μM. MNO$_3$ (M = Na, K, 0.1 mmol) or M(NO$_3$)$_2$ (M = Mn, Co, Ni, Cu, Zn, Cd, Hg, Mg, Ca, Pb and Cr^{3+}, 0.1 mmol) or M(NO$_3$)$_3$ (M = Fe, Al, Ga, In, 0.1 mmol) were separately dissolved in methanol (5 mL). 27 μL of each metal solution (20 mM) were taken and added into 3 mL of each sensor **1** solution (10 μM) prepared above to make 18 equiv. Then, 27 μL of Al(NO$_3$)$_3$ solution (20 mM) were added into the mixed solution of each metal ion and sensor **1** to make 18 equiv. After mixing them for a few seconds, fluorescence spectra were recorded at room temperature.

2.7. Methods for cell imaging and cytotoxicity

Human dermal fibroblast cells in low passage were cultured in FGM-2 medium (Lonza, Switzerland) supplemented with 10% fetal bovine serum, 1% penicillin/streptomycin in an *in vitro* incubator with 5% CO$_2$ at 37 °C. Cells were seeded onto a 12 well plate (SPL Lifesciences, Korea) at a density of 2×10^5 cells per well and then incubated at 37 °C for 4 h after the addition of various concentrations (0–200 μM) of Al(NO$_3$)$_3$ dissolved in DMSO. After washing with phosphate buffered saline (PBS) two times to remove the remaining Al(NO$_3$)$_3$, the cells were incubated with **1** dissolved in a medium/DMSO solution (FGM-2-medium : DMSO = 9 : 1 v/v) at room temperature for 30 min. The cells were observed using a microscope (Olympus, Japan). The fluorescent images of the cells were obtained using a fluorescence microscope (Leica DMLB, Germany) at the excitation wavelength of 410 nm.

To observe cell viability, a live & dead assay was performed for **1** and the **1**-Al^{3+} complex. Fibroblasts (P = 5) were *in vitro* cultured to reach 70% confluence. The cells were incubated with **1** (10 μM) dissolved in a medium/DMSO solution (FGM-2-medium : DMSO = 9 : 1 v/v) for 1 h, 12 h and 24 h, respectively. The reagent (400 μL) of the live & dead assay was added into each cell culture plate. In case of the **1**-Al^{3+} complex, the cells were incubated with Al(NO$_3$)$_3$ (150 μM) dissolved in MeCN. After washing with phosphate buffered saline (PBS) two times to remove the remaining Al(NO$_3$)$_3$, the cells were incubated with **1** dissolved in a medium/DMSO solution (FGM-2-medium : DMSO = 9 : 1 v/v) at room temperature for 1 h, 12 h and 24 h, respectively. The reagent (400 μL) of the live & dead assay was added into each cell culture plate. Both viability and morphological changes of the cells were observed using a fluorescence microscope (Leica DMLB, Leica; Wetzlar, Germany).

2.8. Theoretical calculations

All theoretical calculations were performed by using the Gaussian 03 suite.[66] The singlet ground states (S$_0$) of **1** and the Al^{3+}–2·**1**

complex were optimized by DFT methods with Becke's three parameterized Lee–Yang–Parr (B3LYP) exchange functional[67,68] with the 6-31G** basis set.[69,70] In vibrational frequency calculations, there was no imaginary frequency for **1** and the Al^{3+}–2·**1** complex, suggesting that the optimized **1** and the Al^{3+}–2·**1** complex represented local minima. For all calculations, the solvent effect was considered by using the Cossi and Barone's CPCM (conductor-like polarizable continuum model).[71,72] To investigate the electronic properties of singlet excited states, time-dependent DFT (TDDFT) was performed in the ground state geometries of **1** and the Al^{3+}–2·**1** complex. The 20 singlet–singlet excitations were calculated and analyzed. The GaussSum 2.1[73] was used to calculate the contributions of molecular orbitals in electronic transitions.
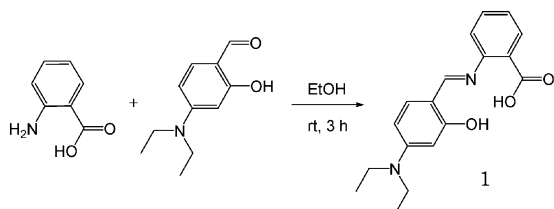
3. Results and discussion

3.1. Spectroscopic measurements of 1 toward Al^{3+}

Sensor **1** was obtained by coupling 2-aminobenzoic acid with 4-(diethylamino)-2-hydroxybenzaldehyde with 74% yield in ethanol (Scheme 1), and characterized by ^{1}H NMR, ESI-mass spectrometry, and elemental analysis.

We studied the fluorescence response behaviors of **1** towards various metal ions in bis-tris buffer (10 mM, pH 7.0, water : CH_3OH = 1 : 1 (v/v)). As shown in Fig. 1, sensor **1** alone displayed a very weak fluorescence emission upon excitation at 410 nm. The addition of Al^{3+} resulted in a prominent fluorescence enhancement (11-fold) at 460 nm. In contrast, other metal ions such as Mn^{2+}, Fe^{3+}, Co^{2+}, Ni^{2+}, Cu^{2+}, Zn^{2+}, Cd^{2+}, Hg^{2+}, Na^+, K^+, Mg^{2+}, Ca^{2+}, Pb^{2+} and Cr^{3+} caused almost no fluorescence increase. Importantly, the addition of Ga^{3+} or In^{3+}, which belong to the same group with Al^{3+} in the periodic table, had no significant effect on the fluorescence, demonstrating that sensor **1** was even highly selective for Al^{3+} over Ga^{3+} and In^{3+}. So far, only a few selective sensors which can discriminate Al^{3+} from both Ga^{3+} and In^{3+} have been reported.[20–22,26] The selectivity of **1** toward Al^{3+} in bis-tris buffer alone was also observed, but fluorescence enhancement was not high enough (Fig. S1, ESI†).

To further study the fluorescence sensing behavior of **1**, a quantitative investigation of the binding affinity of **1** with Al^{3+} was studied by fluorescence titration (Fig. 2). When sensor **1** was titrated with Al^{3+}, the fluorescence intensity increased up to 18 equiv. and then no change was observed, which might be due to a combinational effect of the inhibition of C=N isomerization and the activation of chelation enhanced fluorescence (CHEF).[45,74–76] Imines are poorly fluorescent in part due
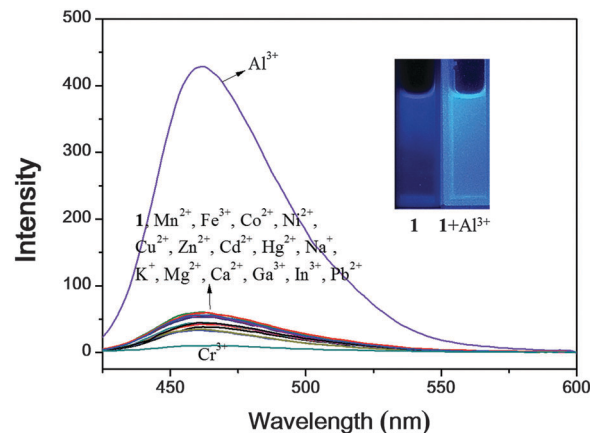

Fig. 1 Fluorescence spectra of sensor **1** (10 μM) upon addition of metal nitrate salts (18 equiv.) of Mn^{2+}, Fe^{3+}, Co^{2+}, Ni^{2+}, Cu^{2+}, Zn^{2+}, Cd^{2+}, Hg^{2+}, Na^+, K^+, Mg^{2+}, Ca^{2+}, Al^{3+}, Ga^{3+}, In^{3+}, Pb^{2+} and Cr^{3+} with an excitation of 410 nm in bis-tris buffer (10 mM, pH 7.0, water : CH_3OH = 1 : 1 (v/v)). Inset: Picture of the fluorescence corresponding to **1** and **1**-Al^{3+} (λ_{ex} = 365 nm).
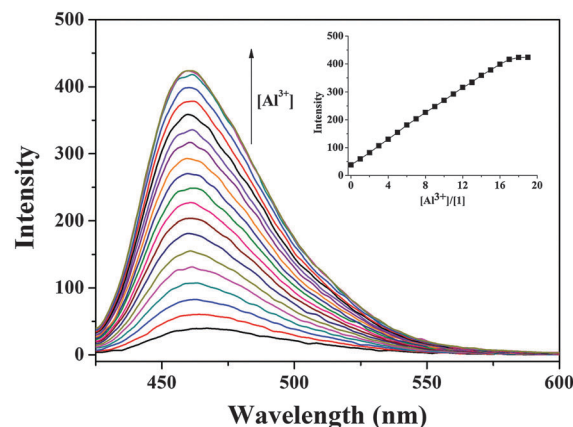

Fig. 2 Fluorescent titration spectra of sensor **1** (10 μM) in the presence of different concentrations of Al^{3+} in bis-tris buffer (10 mM, pH 7.0, water : CH_3OH = 1 : 1 (v/v)). Inset: The fluorescence at 460 nm (λ_{ex} = 410 nm) of **1** as a function of Al^{3+} concentration.

to isomerization of the C=N double bond in the excited state. The C=N isomerization might be inhibited upon complexation with certain metal ions. Therefore, the stable chelation of **1** with Al^{3+} ions made the C=N isomerization of **1** inhibited, resulting in fluorescence enhancement. Moreover, the complexation of **1** with Al^{3+} ions induced rigidity in the resulting molecule and tended to produce a chelation-enhanced fluorescence detection. The fluorescence quantum yields of sensor **1** without and with Al^{3+} were 0.0062 and 0.4240, respectively.[77]

The binding properties of **1** with Al^{3+} were further studied by UV-vis titration experiments (Fig. 3). On treating Al^{3+} with the solution of **1**, the absorption peak at 425 nm gradually decreased while the peak at 352 nm increased. Two clear isosbestic points were observed at 395 and 468 nm, indicative of a clean conversion of **1** into the **1**-Al^{3+} complex.

The Job plot for the binding between **1** and Al^{3+} exhibited a 2 : 1 stoichiometry (Fig. 4).[78] Also, the negative-ion mass spectrum
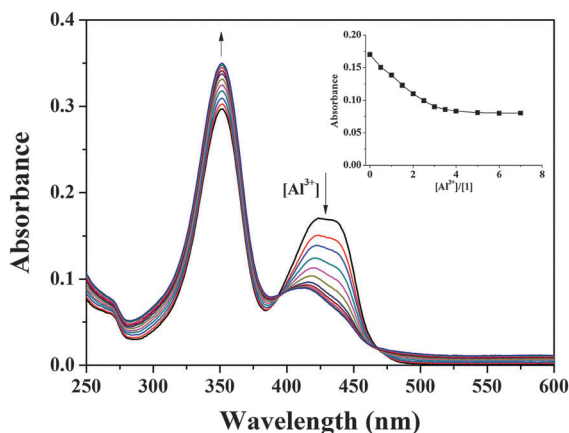

Scheme 1 Synthesis of sensor **1**.

Fig. 3 Absorption spectral changes of **1** (10 μM) in the presence of different concentrations of Al^{3+} ions (5, 10, 15, 20, 25, 30, 35, 40, 50, 60 and 70 μM) in bis-tris buffer (10 mM, pH 7.0, water : CH$_3$OH = 1 : 1 (v/v)). Inset: Absorbance of **1** at 425 nm as a function of Al^{3+} concentration.

for the reaction of **1** with Al^{3+} showed the formation of the [2·**1**(-4H$^+$) + Al^{3+}]$^-$ complex [*m/z*: 647.27; calcd, 647.24] (Fig. S2, ESI†). From the fluorescence titration, the association constant was calculated to be 3.1 × 10^8 M^{-1} from Li's equations (see the ESI,† and Fig. S3).[79] This value is one of the highest binding affinities among such simple Schiff bases for Al^{3+} in buffer solution, indicating that the carboxylic group showed the most effective binding property among other functional groups such as imine, amine, and quinolone (Table S1, ESI†).[80–82]

By using the above-mentioned fluorescence titration results, the detection limit of **1** for the analysis of Al^{3+} ions on the basis of 3σ/K was calculated to be 2.9 × 10^{-7} M (Fig. S4, ESI†).[83] The detection limit of **1** was quite lower than the WHO limit of Al^{3+} (7.41 × 10^{-6} M) acceptable in drinking water, which means that sensor **1** is a powerful tool for the detection of Al^{3+} in aqueous solution. The analytical performance characteristics of the proposed Al^{3+}-sensitive chemosensor were investigated. Fig. 5 shows a calibration curve obtained from the plot of fluorescence
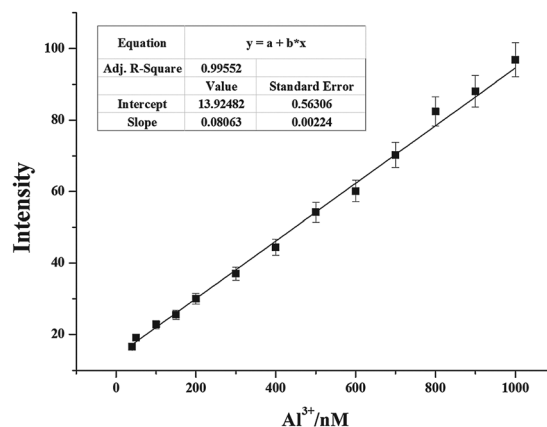

Fig. 5 Calibration curve based on fluorescence intensity with added Al^{3+} concentration.

intensity with the added Al^{3+} concentration. The curve equation was $I = 0.08063C_{Al} + 13.924$ where the C_{Al} unit was nM ($R^2 = 0.996$). The linear range of quantitative detection for aluminum ions was determined to be 40–1000 nM with a detection limit of 290 nM (3σ). The detection limit appeared to be within the range of quantitative detection of aluminum ions. Therefore, sensor **1** was not only selective towards aluminum(III) ions but also possessed a linear response range with a low limit of detection.

The ^{1}H NMR titration experiments of sensor **1** with Al^{3+} ions were studied to further examine the binding mode (Fig. 6). The protons of carboxyl and hydroxyl groups did not appear maybe due to the intra- or inter-molecular hydrogen bonds. Upon addition of 0.5 equiv. of Al^{3+}, the H$_a$ proton of the imine moiety and the H$_c$ and H$_d$ protons of the ethyl groups were shifted to downfield by 0.32, 0.10, and 0.06 ppm, respectively. Also, the protons of the two benzene rings were more complicated and shifted to downfield except for H$_b$, which was shifted to upfield by 0.15 ppm. Further addition of Al^{3+} showed no spectral change. These results suggested that the two oxygen atoms of
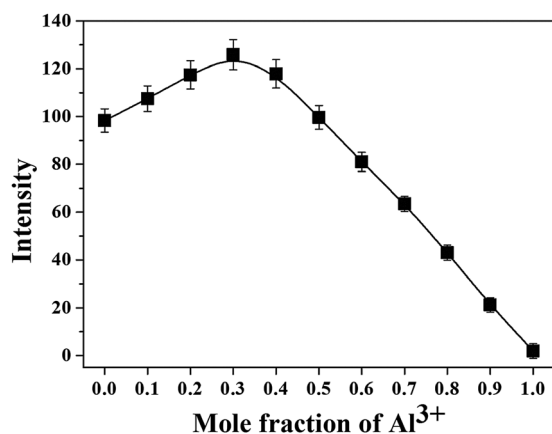

Fig. 4 Job plot of sensor **1** and Al^{3+}, where the intensity at 460 nm was plotted against the mole fraction of aluminum ions. The total concentration of aluminum ions with sensor **1** was 10 μM in bis-tris buffer (10 mM, pH 7.0, water : CH$_3$OH = 1 : 1 (v/v)).
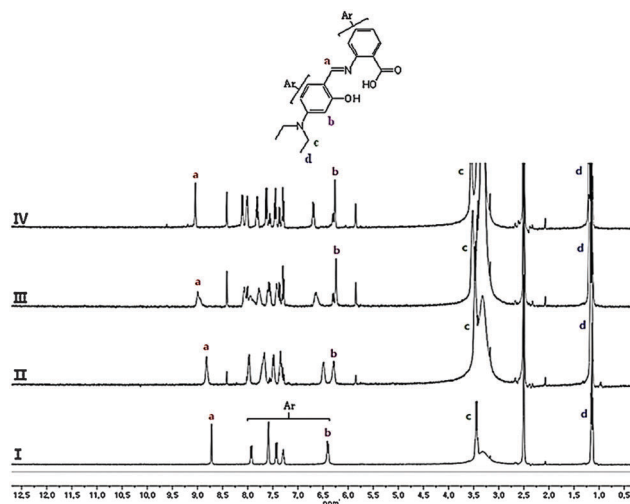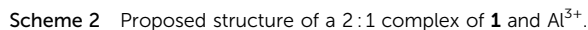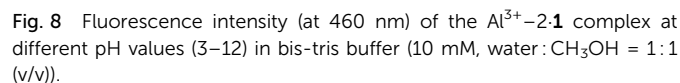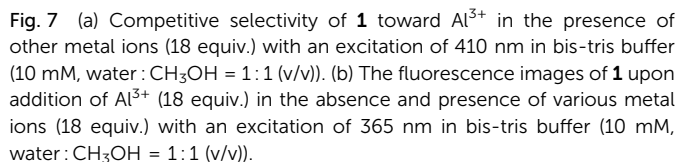

Fig. 6 ^{1}H NMR titration of **1** with Al(NO$_3$)$_3$: (I) **1**; (II) **1** with 0.2 equiv. of Al^{3+}; (III) **1** with 0.5 equiv. of Al^{3+}; and (IV) **1** with 1 equiv. of Al^{3+}.

Scheme 2 Proposed structure of a 2 : 1 complex of **1** and Al^{3+}.

Fig. 8 Fluorescence intensity (at 460 nm) of the Al^{3+}–2·**1** complex at different pH values (3–12) in bis-tris buffer (10 mM, water : CH_3OH = 1 : 1 (v/v)).

the carboxyl and hydroxyl groups and the nitrogen atom of the imine moiety might be involved in Al^{3+} coordination. Based on ^{1}H NMR titration, the Job plot, and ESI-mass spectrometry analysis, we proposed the structure of a 2 : 1 complex of **1** and Al^{3+}, as shown in Scheme 2.

To further check the practical applicability of sensor **1** as an Al^{3+} selective fluorescent sensor, we carried out competition experiments. When **1** was treated with 18 equiv. of Al^{3+} in the presence of the same concentration of other metal ions, the fluorescence enhancement caused by Al^{3+} was retained with Mn^{2+}, Co^{2+}, Ni^{2+}, Zn^{2+}, Cd^{2+}, Hg^{2+}, Na^+, K^+, Mg^{2+}, Ca^{2+}, Ga^{3+}, In^{3+}, and Pb^{2+} (Fig. 7). Instead, Fe^{3+}, Cu^{2+} and Cr^{3+} inhibited about 80%, 80% and 100% of the interaction between **1** and Al^{3+}, which are the well known strong quenchers of fluorescence.[84,85]

Thus, sensor **1** can be used as a selective fluorescent sensor for Al^{3+} in the presence of most competing metal ions.

For biological applications, the pH dependence of the Al^{3+}–2·**1** complex was examined in bis-tris buffer (10 mM, water : CH_3OH = 1 : 1 (v/v)) solution (Fig. 8). The fluorescence intensity of the Al^{3+}–2·**1** complex displayed a significant response between pH 5 and 10, which includes the environmentally relevant range of pH 7.0–8.4.[86] These results indicated that Al^{3+} could be clearly detected by the fluorescence spectra measurement using **1** over the environmentally relevant pH range (pH 7.0–8.4).

3.2. Application for cell imaging

Further experiments were conducted to test whether intracellular Al^{3+} could be monitored by fluorimetry. Adult human dermal fibroblasts were first incubated with various concentrations of Al^{3+} (0, 30, 50, 100, 150 and 200 μM) for 4 h and then exposed to **1** for 30 min before imaging, so that **1** could permeate easily through the living cells without any harm. The fibroblasts that were cultured with both Al^{3+} and **1** exhibited fluorescence (Fig. 9), whereas the cells cultured without Al^{3+} or **1** did not exhibit fluorescence. The intensity and region of the fluorescence within the cell containing **1** gradually increased with an increase in the Al^{3+} concentration from 0 to 200 μM and the fluorescence intensity of the cells persisted even after 5 h from exposure to **1**. Moreover, the biocompatibility of **1** was also examined with the living cells (Fig. S5, ESI†). All the fibroblasts were still alive for 24 h. These results showed that the new sensor **1** was efficient to image Al^{3+} in cells, and could be useful in the determination of the exposure level of cells to Al^{3+}.

3.3. Theoretical calculations for 1 and the Al^{3+}–2·1 complex

To gain an insight into the fluorescent sensing mechanism for the Al^{3+}–2·**1** complex, time-dependent density functional theory (TD-DFT) calculations were performed at the optimized geometries (S_0) of **1** and the Al^{3+}–2·**1** complex (Fig. S6, ESI†). The optimized geometries were calculated based on the Job plot, ESI-mass and ^{1}H NMR titration. In case of **1**, the main molecular
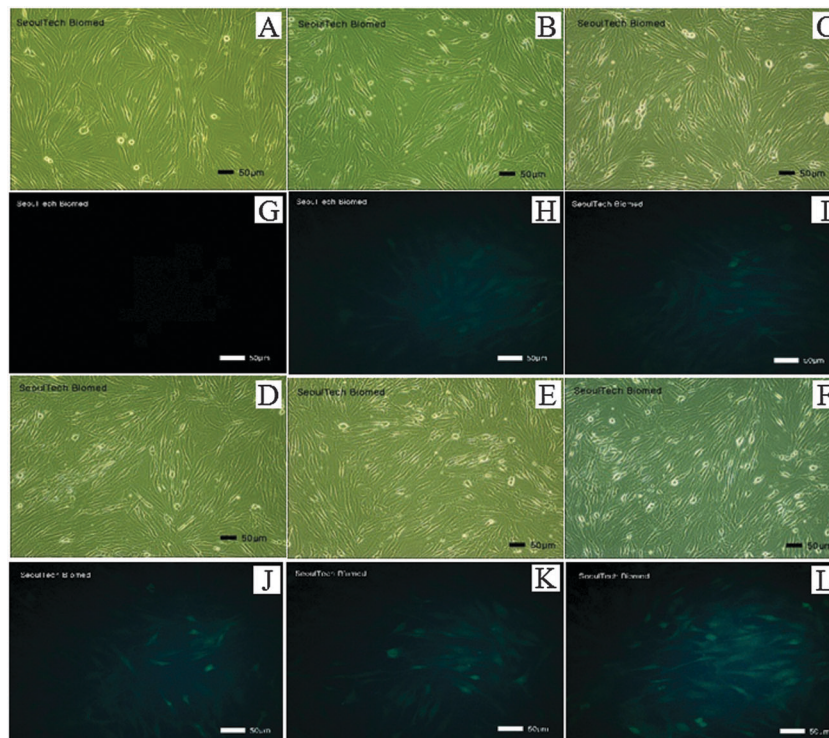

Fig. 7 (a) Competitive selectivity of **1** toward Al^{3+} in the presence of other metal ions (18 equiv.) with an excitation of 410 nm in bis-tris buffer (10 mM, water : CH_3OH = 1 : 1 (v/v)). (b) The fluorescence images of **1** upon addition of Al^{3+} (18 equiv.) in the absence and presence of various metal ions (18 equiv.) with an excitation of 365 nm in bis-tris buffer (10 mM, water : CH_3OH = 1 : 1 (v/v)).

Fig. 9 Fluorescence images of fibroblasts cultured with Al^{3+} and **1**. Cells were exposed to 0 (A and G), 30 (B and H), 50 (C and I), 100 (D and J), 150 (E and K) and 200 μM (F and L) Al(NO$_3$)$_3$ for 4 h and then later with **1** for 30 min. The images (A–F) were observed using a light microscope and the images (G–L) were taken using a fluorescence microscope. The scale bar is 50 μm.

orbital (MO) contribution of the first lowest excited state was determined for the HOMO → LUMO transition (394.61 nm, Fig. S7, ESI†), which indicated an intramolecular charge transfer (ICT) transition from the julolidine moiety to the benzoic acid moiety. For the Al^{3+}–2·**1** complex, the first lowest excited state was determined for the HOMO → LUMO transition (499.43 nm, Fig. S8, ESI†), which indicated the forbidden transition (oscillator strength: 0.0045). The main molecular orbital (MO) contributions of the fifth lowest excited states were determined for HOMO → LUMO+1 and HOMO−1 → LUMO+1 transitions (367.42 nm, Fig. S8, ESI†), which showed the allowed transition and was similar to the intramolecular charge transfer (ICT) transition of **1**. There were no obvious changes in the electronic transitions between **1** and the Al^{3+}–2·**1** complex. Only, hypochromic shift (394.61 to 367.42 nm) was observed upon chelation of **1** with Al^{3+}. These results suggested that the sensing mechanism of **1** toward Al^{3+} originated from the rigid structure of the Al^{3+}–2·**1** complex, which might inhibit the non-radiative process such as C=N isomerization. Thus, the CHEF effect and the inhibition of C=N isomerization plays an important role in fluorescence enhancement.[87,88]

4. Conclusion

We have developed a simple, cost-effective, fluorescent aminobenzoic acid-based chemosensor **1** for selective determination of Al^{3+} in aqueous solution. Sensor **1** displayed a remarkable fluorescence enhancement in the presence of Al^{3+} ions and can

be successfully applied to living cells for detecting Al^{3+}. The large enhancement of fluorescence was explained by the inhibition of C=N isomerization and the activation of chelation enhanced fluorescence (CHEF), which were explained by theoretical calculations. On the basis of the Job plot, ^{1}H NMR titration and ESI-mass spectrometry analysis, the formation of the 2 : 1 (**1** : M) complex was proposed. Moreover, sensor **1** showed one of the highest binding constants (3.1×10^8) among such simple Schiff bases in aqueous solution and displayed a linear response range with a low limit of detection (290 nM) for the analytical performance of Al^{3+} ions.

References

1 C. Liang, W. Bu, C. Li, G. Men, M. Deng, Y. Jiangyao, H. Sun and S. Jiang, *Dalton Trans.*, 2015, **44**, 11352–11359.
2 H. Wang, B. Wang, Z. Shi, X. Tang, W. Dou, Q. Han, Y. Zhang and W. Liu, *Biosens. Bioelectron.*, 2015, **65**, 91–96.
3 C. Li, J. Qin, G. Wang, B. Wang, A. Fu and Z. Yang, *Inorg. Chim. Acta*, 2015, **430**, 91–95.

4 R. R. Koner, S. Sinha, S. Kumar, C. K. Nandi and S. Ghosh, *Tetrahedron Lett.*, 2012, **53**, 2302–2307.

5 S. Sinha, T. Mukherjee, J. Mathew, S. K. Mukhopadhyay and S. Ghosh, *Anal. Chim. Acta*, 2014, **822**, 60–68.

6 Z. Liu, C. Zhang, Y. Li, Z. Wu, F. Qian, X. Yang, W. He, X. Gao and Z. Guo, *Org. Lett.*, 2009, **11**, 795–798.

7 X. Qu, C. Li, H. Chen, J. Mack, Z. Guo and Z. Shen, *Chem. Commun.*, 2013, **49**, 7510–7512.

8 D. Maity and T. Govindaraju, *Inorg. Chem.*, 2010, **49**, 7229–7231.

9 D. Maity and T. Govindaraju, *Chem. Commun.*, 2010, **46**, 4499–4501.

10 A. Sahana, A. Banerjee, S. Lohar, A. Banik, S. K. Mukhopadhyay, D. A. Safin, M. G. Babashkina, M. Bolte, Y. Garcia and D. Das, *Dalton Trans.*, 2013, **42**, 13311–13314.

11 A. Banerjee, A. Sahana, S. Das, S. Lohar, B. Sarkar, S. K. Mukhopadhyay, A. K. Mukherjee and D. Das, *Analyst*, 2012, **137**, 2166–2175.

12 J. Y. Jung, S. J. Han, J. Chun, C. Lee and J. Yoon, *Dyes Pigm.*, 2012, **94**, 423–426.

13 S. Yun, Y.-O. Kim, D. Kim, H. G. Kim, H. Ihm, J. K. Kim, C.-W. Lee, W. J. Lee, J. J. Yoon, K. S. Oh, J. Yoon, S.-M. Park and K. S. Kim, *Org. Lett.*, 2003, **5**, 471–474.

14 G. Berthon, *Coord. Chem. Rev.*, 2002, **228**, 319–341.

15 Z. Krejpcio and R. W. Wojciak, *Pol. J. Environ. Stud.*, 2002, **11**, 251–254.

16 J. Barcelo and C. Poschenrieder, *Environ. Exp. Bot.*, 2002, **48**, 75–92.

17 P. Nayak, *Environ. Res.*, 2002, **89**, 101–115.

18 J. Kumar, M. J. Sarma and P. Phukan, *Dalton Trans.*, 2015, **44**, 4576–4581.

19 C. Exley, *Coord. Chem. Rev.*, 2012, **256**, 2142–2146.

20 J. Lee, H. Kim, S. Kim, J. Y. Noh, E. J. Song, C. Kim and J. Kim, *Dyes Pigm.*, 2013, **96**, 590–594.

21 M. Mukherjee, S. Pal, S. Lohar, B. Sen, S. Sen, S. Banerjee and P. Chattopadhyay, *Analyst*, 2014, **139**, 4828–4835.

22 S. Hu, J. Song, G. Wu, C. Cheng and Q. Gao, *Spectrochim. Acta, Part A*, 2014, **136**, 1188–1194.

23 Y. J. Jang, Y. H. Yeon, H. Y. Yang, J. Y. Noh, I. H. Hwang and C. Kim, *Inorg. Chem. Commun.*, 2013, **33**, 48–51.

24 L. Wang, L. Yang and D. Cao, *Sens. Actuators, B*, 2014, **202**, 949–958.

25 W. Cao, X.-J. Zheng, J.-P. Sun, W.-T. Wong, D.-C. Fang, J.-X. Zhang and L.-P. Jin, *Inorg. Chem.*, 2014, **53**, 3012–3021.

26 J. Y. Noh, S. Kim, I. H. Hwang, G. Y. Lee, J. Kang, S. H. Kim, J. Min, S. Park, C. Kim and J. Kim, *Dyes Pigm.*, 2013, **99**, 1016–1021.

27 K. Tiwari, M. Mishra and V. P. Singh, *RSC Adv.*, 2013, **3**, 12124–12132.

28 C.-H. Chen, D.-J. Liao, C.-F. Wan and A.-T. Wu, *Analyst*, 2013, **138**, 2527–2530.

29 S. Kim, J. Y. Noh, K. Y. Kim, J. H. Kim, H. K. Kang, S. W. Nam, S. H. Kim, S. Park, C. Kim and J. Kim, *Inorg. Chem.*, 2012, **51**, 3597–3602.

30 L. Fan, J. Qin, T. Li, B. Wang and Z. Yang, *Sens. Actuators, B*, 2014, **203**, 550–556.

31 Y. K. Jang, U. C. Nam, H. L. Kwon, I. H. Hwang and C. Kim, *Dyes Pigm.*, 2013, **99**, 6–13.

32 O. Alici and S. Erdemir, *Sens. Actuators, B*, 2015, **208**, 159–163.

33 Y. Jiang, L.-L. Sun, G.-Z. Ren, X. Niu, W.-Z. Hu and Z.-Q. Hu, *ChemistryOpen*, 2015, **4**, 378–382.

34 S. Erdemir, O. Kocyigit and S. Malkondu, *J. Fluoresc.*, 2015, **25**, 719–727.

35 N. R. Chereddy, P. Nagaraju, M. V. N. Raju, V. R. Krishnaswamy, P. S. Korrapati, P. R. Bangal and V. J. Rao, *Biosens. Bioelectron.*, 2015, **68**, 749–756.

36 S. Gui, Y. Huang, F. Hu, Y. Jin, G. Zhang, L. Yan, D. Zhang and R. Zhao, *Anal. Chem.*, 2015, **87**, 1470–1474.

37 L. Peng, Z. Zhou, X. Wang, R. Wei, K. Li, Y. Xiang and A. Tong, *Anal. Chim. Acta*, 2014, **829**, 54–59.

38 S. K. Shooraa, A. K. Jaina and V. K. Gupta, *Sens. Actuators, B*, 2015, **216**, 86–104.

39 H. Kim, B. A. Rao, J. W. Jeong, S. Mallick, S.-M. Kang, J. S. Choi, C.-S. Lee and Y.-A. Son, *Sens. Actuators, B*, 2015, **210**, 173–182.

40 J. W. Jeong, B. A. Rao and Y.-A. Son, *Sens. Actuators, B*, 2015, **208**, 75–84.

41 W.-H. Ding, D. Wang, X.-J. Zheng, W.-J. Ding, J.-Q. Zheng, W.-H. Mu, W. Cao and L.-P. Jin, *Sens. Actuators, B*, 2015, **209**, 359–367.

42 S. Paul, A. Manna and S. Goswami, *Dalton Trans.*, 2015, **44**, 11805–11810.

43 J. Wang and Y. Pang, *RSC Adv.*, 2014, **4**, 5845–5848.

44 S. Goswami, A. Manna, S. Paul, A. K. Maity, P. Saha, C. K. Quah and H.-K. Fun, *RSC Adv.*, 2014, **4**, 34572–34576.

45 J. J. Lee, G. J. Park, Y. S. Kim, S. Y. Lee, H. J. Lee, I. S. Noh and C. Kim, *Biosens. Bioelectron.*, 2015, **69**, 226–229.

46 Y. Lu, S. Huang, Y. Liu, S. He, L. Zhao and X. Zeng, *Org. Lett.*, 2011, **13**, 5274–5277.

47 S. H. Kim, H. S. Choi, J. Kim, S. J. Lee, D. T. Quang and J. S. Kim, *Org. Lett.*, 2012, **12**, 560–563.

48 S. Sen, T. Mukherjee, B. Chattopadhyay, A. Moirangthem, A. Basu, J. Marek and P. Chattopadhyay, *Analyst*, 2012, **137**, 3975–3981.

49 V. P. Singh, K. Tiwari, M. Mishra, N. Srivastava and S. Saha, *Sens. Actuators, B*, 2013, **182**, 546–554.

50 S. Guha, S. Lohar, A. Sahana, A. Banerjee, D. A. Safin, M. G. Babashkina, M. P. Mitoraj, M. Bolte, Y. Garcia, S. K. Mukhopadhyay and D. Das, *Dalton Trans.*, 2013, **42**, 10198–10207.

51 S. Das, A. Sahana, A. Banerjee, S. Lohar, D. A. Safin, M. G. Babashkina, M. Bolte, Y. Garcia, I. Hauli, S. K. Mukhopadhyay and D. Das, *Dalton Trans.*, 2013, **42**, 4757–4763.

52 A. Sahana, A. Banerjee, S. Das, S. Lohar, D. Karak, B. Sarkar, S. K. Mukhopadhyay, A. K. Mukherjee and D. Das, *Org. Biomol. Chem.*, 2011, **9**, 5523–5529.

53 L. Wang, W. Qin, X. Tang, W. Dou, W. Liu, Q. Teng and X. Yao, *Org. Biomol. Chem.*, 2010, **8**, 3751–3757.

54 S. Sinha, R. R. Koner, S. Kumar, J. Mathew, P. V. Monisha, I. Kazi and S. Ghosh, *RSC Adv.*, 2013, **3**, 345–351.

55 Y.-W. Wang, M.-X. Yu, Y.-H. Yu, Z.-P. Bai, Z. Shen, F.-Y. Li and X.-Z. You, *Tetrahedron Lett.*, 2009, **50**, 6169–6172.

56 A. Dhara, A. Jana, S. Konar, S. K. Ghatak, S. Ray, K. Das, A. Bandyopadhyay, N. Guchhait and S. K. Kar, *Tetrahedron Lett.*, 2013, **54**, 3630–3634.

57 T.-J. Jia, W. Cao, X.-J. Zheng and L.-P. Jin, *Tetrahedron Lett.*, 2013, **54**, 3471–3474.

58 B. K. Datta, C. Kar, A. Basu and G. Das, *Tetrahedron Lett.*, 2013, **54**, 771–774.

59 D. Karak, S. Lohar, A. Sahana, S. Guha, A. Banerjee and D. Das, *Anal. Methods*, 2012, **4**, 1906–1908.

60 K. Kaur, V. K. Bhardwaj, N. Kaur and N. Singh, *Inorg. Chem. Commun.*, 2012, **26**, 31–36.

61 Z. Liu, Z. Yang, Y. Li, T. Li, B. Wang, Y. Li and X. Jin, *Inorg. Chim. Acta*, 2013, **395**, 77–80.

62 J. Isaad and A. E. Achari, *Tetrahedron*, 2011, **67**, 4939–4947.

63 S. Mukherjee, P. Mal and H. Stoeckli-Evans, *J. Lumin.*, 2014, **155**, 185–190.

64 Z. Yu, L. A. Bracero, L. Chen, W. Song, X. Wang and B. Zhao, *Spectrochim. Acta, Part A*, 2013, **105**, 52–56.

65 Z. Li, J. Pan and J. Tang, *Anal. Lett.*, 2002, **35**, 167–183.

66 M. J. Frisch, G. W. Trucks, H. B. Schlegel, G. E. Scuseria, M. A. Robb, J. R. Cheeseman, J. A. Montgomery, Jr., T. Vreven, K. N. Kudin, J. C. Burant, J. M. Millam, S. S. Iyengar, J. Tomasi, V. Barone, B. Mennucci, M. Cossi, G. Scalmani, N. Rega, G. A. Petersson, H. Nakatsuji, M. Hada, M. Ehara, K. Toyota, R. Fukuda, J. Hasegawa, M. Ishida, T. Nakajima, Y. Honda, O. Kitao, H. Nakai, M. Klene, X. Li, J. E. Knox, H. P. Hratchian, J. B. Cross, V. Bakken, C. Adamo, J. Jaramillo, R. Gomperts, R. E. Stratmann, O. Yazyev, A. J. Austin, R. Cammi, C. Pomelli, J. W. Ochterski, P. Y. Ayala, K. Morokuma, G. A. Voth, P. Salvador, J. J. Dannenberg, V. G. Zakrzewski, S. Dapprich, A. D. Daniels, M. C. Strain, O. Farkas, D. K. Malick, A. D. Rabuck, K. Raghavachari, J. B. Foresman, J. V. Ortiz, Q. Cui, A. G. Baboul, S. Clifford, J. Cioslowski, B. B. Stefanov, G. Liu, A. Liashenko, P. Piskorz, I. Komaromi, R. L. Martin, D. J. Fox, T. Keith, M. A. Al-Laham, C. Y. Peng, A. Nanayakkara, M. Challacombe, P. M. W. Gill, B. Johnson, W. Chen, M. W. Wong, C. Gonzalez and J. A. Pople, *Gaussian 03, Revision D.01*, Gaussian, Inc., Wallingford CT, 2004.

67 A. D. Becke, *J. Chem. Phys.*, 1993, **98**, 5648–5652.

68 C. Lee, W. Yang and R. G. Parr, *Phys. Rev. B: Condens. Matter Mater. Phys.*, 1988, **37**, 785–789.

69 P. C. Hariharan and J. A. Pople, *Theor. Chim. Acta*, 1973, **28**, 213–222.

70 M. M. Francl, W. J. Petro, W. J. Hehre, J. S. Binkley, M. S. Gordon, D. F. DeFrees and J. A. Pople, *J. Chem. Phys.*, 1982, **77**, 3654–3665.

71 V. Barone and M. Cossi, *J. Phys. Chem. A*, 1998, **102**, 1995–2001.

72 M. Cossi and V. Barone, *J. Chem. Phys.*, 2001, **115**, 4708–4717.

73 N. M. O'Boyle and A. L. Tenderholt, *J. Comput. Chem.*, 2008, **29**, 839–845.

74 L. Wang, W. Qin, X. Tang, W. Dou and W. J. Liu, *J. Phys. Chem. A*, 2011, **115**, 1609–1616.

75 S. A. Lee, G. R. You, Y. W. Choi, H. Y. Jo, A. R. Kim, I. Noh, S.-J. Kim, Y. Kim and C. Kim, *Dalton Trans.*, 2014, **43**, 6650–6659.

76 Y. W. Choi, G. J. Park, Y. J. Na, H. Y. Jo, S. A. Lee, G. R. You and C. Kim, *Sens. Actuators, B*, 2014, **194**, 343–352.

77 S. C. Burdette, G. K. Walkup, B. Spingler, R. Y. Tsien and S. J. Lippard, *J. Am. Chem. Soc.*, 2011, **123**, 7831–7841.

78 P. Job, *Ann. Chim.*, 1928, **9**, 113–203.

79 R. Yang, K. Li, K. Wang, F. Zhao, N. Li and F. Liu, *Anal. Chem.*, 2003, **75**, 612–621.

80 F. Yu, L. J. Hou, L. Y. Qin, J. B. Chao, Y. Wang and W. J. Jin, *J. Photochem. Photobiol., A*, 2016, **315**, 8–13.

81 J. Qin, Z. Yang and P. Yang, *Inorg. Chim. Acta*, 2015, **432**, 136–141.

82 W.-H. Ding, D. Wang, X.-J. Zheng, W.-J. Ding, J.-Q. Zheng, W.-H. Mu, W. Cao and L.-P. Jin, *Sens. Actuators, B*, 2015, **209**, 359–367.

83 Y.-K. Tsui, S. Devaraj and Y.-P. Yen, *Sens. Actuators, B*, 2012, **161**, 510–519.

84 B. Bodenant, F. Fages and M.-H. Delville, *J. Am. Chem. Soc.*, 1998, **120**, 7511–7519.

85 A. Torrado, G. K. Walkup and B. Imperiali, *J. Am. Chem. Soc.*, 1998, **120**, 609–610.

86 R. M. Harrison, D. P. H. Laxen and S. J. Wilson, *Environ. Sci. Technol.*, 1981, **15**, 1378–1383.

87 D. Maity and T. Govindaraju, *Eur. J. Inorg. Chem.*, 2011, 5479–5485.

88 D. Maity and T. Govindaraju, *Chem. Commun.*, 2012, **48**, 1039–1041.